

Short communication

Synthesis and electrochemical properties of layered $\text{Li}[\text{Ni}_{0.333}\text{Co}_{0.333}\text{Mn}_{0.293}\text{Al}_{0.04}]\text{O}_{2-z}\text{F}_z$ cathode materials prepared by the sol–gel method

Li Liao^a, Xianyou Wang^{a,*}, Xufang Luo^a, Ximing Wang^a, Sergio Gamboa^b, P.J. Sebastian^b

^a College of Chemistry, Xiangtan University, Hunan 411105, PR China

^b Solar-Hydrogen-Fuel Cell Group, CIE-UNAM, Temixco 62580, Morelos, Mexico

Received 18 December 2005; accepted 31 December 2005

Available online 31 March 2006

Abstract

The cathode-active materials, layered $\text{Li}[\text{Ni}_{0.333}\text{Co}_{0.333}\text{Mn}_{0.293}\text{Al}_{0.04}]\text{O}_{2-z}\text{F}_z$ ($0 \leq z \leq 0.1$), were synthesized from a sol–gel precursor at 900 °C in air. The influence of Al–F co-substitution on the structural and electrochemical properties of the as-prepared samples was characterized by X-ray diffraction (XRD), scanning electron microscope (SEM) and electrochemical experiments. The results showed that $\text{Li}[\text{Ni}_{0.333}\text{Co}_{0.333}\text{Mn}_{0.293}\text{Al}_{0.04}]\text{O}_{2-z}\text{F}_z$ has a typical hexagonal structure with a single phase, the particle sizes of the samples tended to increase with increasing fluorine content. It has been found that $\text{Li}[\text{Ni}_{0.333}\text{Co}_{0.333}\text{Mn}_{0.293}\text{Al}_{0.04}]\text{O}_{1.95}\text{F}_{0.05}$ showed an improved cathodic behavior and discharge capacity retention compared to the undoped samples in the voltage range of 3.0–4.3 V. The electrodes prepared from $\text{Li}[\text{Ni}_{0.333}\text{Co}_{0.333}\text{Mn}_{0.293}\text{Al}_{0.04}]\text{O}_{1.95}\text{F}_{0.05}$ delivered an initial discharge capacity of 158 mAh^{-1}g and an initial coulombic efficiency is 91.3%, and the capacity retention at the 20th cycle was 94.9%. Though the F-doped samples had lower initial capacities, they showed better cycle performances compared with F-free samples. Therefore, this is a promising material for a lithium-ion battery.

© 2006 Elsevier B.V. All rights reserved.

Keywords: Lithium-ion battery; Cathode materials; Al–F co-substitution; Capacity retention

1. Introduction

In the recent years, the layered transition metal oxide $\text{Li}(\text{Ni}_{1/3}\text{Co}_{1/3}\text{Mn}_{1/3})\text{O}_2$ has attracted much attention due to its high capacity, good cycling performance and thermal stability [1–3]. It has a typical hexagonal $\alpha\text{-NaFeO}_2$ structure with a space group of $R\bar{3}m$, and the oxidation states of Ni, Co and Mn in the compound are 2+, 3+ and 4+, respectively [4]. The electrochemical processes involve the oxidation of Ni^{2+} to Ni^{4+} during the initial stage and Co^{3+} to Co^{4+} in a later stage [5]. Ohzuku and co-workers synthesized $\text{Li}(\text{Ni}_{1/3}\text{Co}_{1/3}\text{Mn}_{1/3})\text{O}_2$ in 2001 for the first time, which delivered a stable capacity of 150 mAh^{-1}g in the voltage range 2.5–4.2 V with excellent cyclability [6]. Shaju et al. reported this material possessed a

discharge capacity of 215 mAh^{-1}g when cycled between 2.5 and 4.7 V [7]. It is considered to be one of the most promising cathode materials for a lithium-ion battery to replace LiCoO_2 . However, further improvement is needed for its suitability to practical uses such as high-energy and power density. Small amounts of additional dopants like Mg [8], F [9], Mo [10] and Si [11] into the $\text{Li}(\text{Ni}_{1/3}\text{Co}_{1/3}\text{Mn}_{1/3})\text{O}_2$ lattice have been reported to improve structural stability and enhance the cycling performance. Jouanneau et al. discussed the influence of LiF additions on $\text{Li}[\text{Ni}_x\text{Co}_{1-2x}\text{Mn}_x]\text{O}_2$ and found that materials could be obtained using LiF as a sintering agent with almost no disturbance of the cell performance [12]. Mg–F co-substitution into $\text{Li}(\text{Ni}_{1/3}\text{Co}_{1/3}\text{Mn}_{1/3})\text{O}_2$ have been observed by Kim [13]. Co-doping was effective for the improvement of physical properties, which enhanced the capacity and thermal stability, even though the cells were cycled between 2.8–4.6 V [13].

In this paper, we synthesized Al–F co-doped $\text{Li}[\text{Ni}_{0.333}\text{Co}_{0.333}\text{Mn}_{0.293}\text{Al}_{0.04}]\text{O}_{2-z}\text{F}_z$ ($0 \leq z \leq 0.1$) materials by the

* Corresponding author. Tel.: +86 732 8293371; fax: +86 732 8292061.
E-mail address: wxianyou@yahoo.com (X. Wang).

sol–gel method using citric acid as a chelating agent combined with a high calcination process. The effects of Al–F co-substitution on the structural, electrochemical performance of $\text{Li}(\text{Ni}_{1/3}\text{Co}_{1/3}\text{Mn}_{1/3})\text{O}_2$ compounds were studied in detail.

2. Experimental

Al–F co-substituted $\text{Li}[\text{Ni}_{0.333}\text{Co}_{0.333}\text{Mn}_{0.293}\text{Al}_{0.04}]\text{O}_{2-z}\text{F}_z$ ($0 \leq z \leq 0.1$) powders were prepared using a sol–gel method with citric acid as chelating agent. Lithium nitrate ($\text{LiNO}_3 \cdot \text{H}_2\text{O}$), lithium fluoride (LiF), nickel nitrate ($\text{Ni}(\text{NO}_3)_2 \cdot 6\text{H}_2\text{O}$), cobalt nitrate ($\text{Co}(\text{NO}_3)_2 \cdot 6\text{H}_2\text{O}$), aluminum nitrate ($\text{Al}(\text{NO}_3)_3 \cdot 9\text{H}_2\text{O}$) and manganese nitrate ($\text{Mn}(\text{NO}_3)_2 \cdot 4\text{H}_2\text{O}$) were used as the starting materials. A stoichiometric amount of metal nitrates and LiF were dissolved in distilled water, and then added drop wise to a continuously stirred aqueous solution of citric acid. The molar ratio of citric acid to total metal ions was 2:1. The solution was subsequently adjusted to pH 8–9 by ammonium hydroxide. The resultant solution was evaporated at 70–80 °C to form a transparent gel. The gel was dried at 120 °C for 12 h to get the precursor powders. These precursors were heated at 480 °C for 5 h in air in order to eliminate the organic residues. The product was ground thoroughly in an agate mortar and pressed into pellets. These pellets were recalcined at 900 °C for 18 h, followed by quenching to room temperature.

Powder X-ray diffraction (D/max-2550 Rigaku, Japan) measurement using Cu $K\alpha$ radiation was employed to identify the crystal structure of products. The morphology and particle sizes of products were performed via scanning electron microscope (SEM) using a JEOL Microscope.

The laboratory cells consisted of a cathode and a lithium metal anode separated by a Celgard 2400 porous polypropylene film. The positive electrodes were fabricated with active $\text{Li}[\text{Ni}_{0.333}\text{Co}_{0.333}\text{Mn}_{0.293}\text{Al}_{0.04}]\text{O}_{2-z}\text{F}_z$ powders, carbon black and colloidal PTFE binder in the weight ratio of 75:15:10. The mixture was pressed onto a stainless steel mesh at a pressure of 18 MPa, then dried under vacuum at 120 °C for 12 h. The electrolyte was 1 M LiPF_6 in EC-DMC (1:1 in volume). The cell was assembled in an argon-filled dry box and tested at room temperature (25 °C). Electrochemical tests were performed on the cell at a current density of $16 \text{ mA}^{-1} \text{ g}$ (0.1 C) with cut-off voltages of 3.0–4.3 V.

3. Results and discussion

Fig. 1 shows X-ray diffraction patterns of the $\text{Li}[\text{Ni}_{0.333}\text{Co}_{0.333}\text{Mn}_{0.293}\text{Al}_{0.04}]\text{O}_{2-z}\text{F}_z$ ($0 \leq z \leq 0.1$) powders prepared by heating the precursor at 900 °C for 18 h in air. All samples could be indexed based on the hexagonal $\alpha\text{-NaFeO}_2$ structure type (space group: $R\bar{3}m$) and no impurity-related peaks are observed. It indicates that synthesized samples were single phase and formed a layered crystal structure in the range of $z=0$ –0.1. In XRD patterns, the (006)/(102) and (108)/(110) peak pairs were clearly split, which means that samples with highly hexagonal layered ordering were formed [14]. The integrated intensity ratio of the (003) and (104) peak is used to measure the degree of cation mixing in the layer structure. For I_{003}/I_{104} value is less

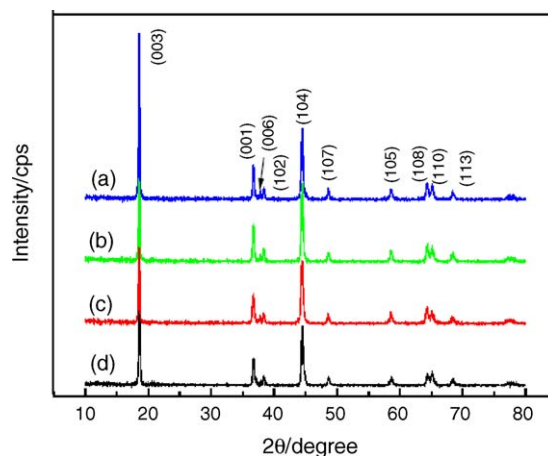


Fig. 1. X-ray diffraction pattern of $\text{Li}[\text{Ni}_{0.333}\text{Co}_{0.333}\text{Mn}_{0.293}\text{Al}_{0.04}]\text{O}_{2-z}\text{F}_z$ powders, prepared at 900 °C for 18 h in air: (a) $z=0$, (b) $z=0.02$, (c) $z=0.05$ (d) $z=0.1$.

than 1.2, undesirable cation mixing takes place [15,16]. The I_{003}/I_{104} value of $\text{Li}[\text{Ni}_{0.333}\text{Co}_{0.333}\text{Mn}_{0.293}\text{Al}_{0.04}]\text{O}_2$ (1.58) was higher than that of $\text{Li}(\text{Ni}_{1/3}\text{Co}_{1/3}\text{Mn}_{1/3})\text{O}_2$ (1.25) reported by Li and co-workers [2]. Because the radius of Ni^{2+} (0.69 Å) and Li^+ (0.76 Å) are similar, displacement between the transition metal ions at the 3a sites and lithium ions at 3b sites would give rise to cation mixing in the structure [17,18]. A small amount of Al substitution for transition metals could prevent occupancy of the Li^+ layers by Ni^{2+} , which is beneficial for the performance during electrochemical cycling [19]. However, the I_{003}/I_{104} value of F-doped samples was monotonously decreased to 1.36 as the fluorine content increased, which indicates that some cation mixing occurred in the crystal lattice.

The lattice parameters and structural parameters were calculated and summarized in Table 1. The lattice parameters of the F-free sample $\text{Li}[\text{Ni}_{0.333}\text{Co}_{0.333}\text{Mn}_{0.293}\text{Al}_{0.04}]\text{O}_2$ ($z=0$) were calculated to be $a=2.862 \text{ Å}$, $c=14.249 \text{ Å}$ and $V=101.09 \text{ Å}^3$. Compared with the values of $\text{Li}(\text{Ni}_{1/3}\text{Co}_{1/3}\text{Mn}_{1/3})\text{O}_2$ observed by Wang et al. ($a=2.885 \text{ Å}$, $c=14.306 \text{ Å}$, $V=103.12 \text{ Å}^3$) [20] and Tong et al. ($a=2.872 \text{ Å}$, $c=14.243 \text{ Å}$, $V=101.74 \text{ Å}^3$) [21], the lattice parameters are slightly decreased in both a - and c -axis. The smaller ionic size of Al^{3+} (0.50 Å) compared to that of Mn^{4+} (0.54 Å³) might offer the lattice parameters in the layered structure. As the fluorine content increased, the lattice parameter increased monotonously, and the cell volume also increased from 101.09 Å^3 for $z=0$ to 101.68 Å^3 for $z=0.1$. Although the radii of F^- anions (1.33 Å) is smaller than that of O^{2-} (1.40 Å),

Table 1
Lattice parameters and structural parameters for $\text{Li}[\text{Ni}_{0.333}\text{Co}_{0.333}\text{Mn}_{0.293}\text{Al}_{0.04}]\text{O}_{2-z}\text{F}_z$

z	$a(\text{Å})$	$c(\text{Å})$	cla	I_{003}/I_{104}	Unit cell volume (Å^3)
0	2.862	14.249	4.979	1.58	101.09
0.02	2.863	14.250	4.977	1.53	101.16
0.05	2.866	14.252	4.973	1.45	101.37
0.1	2.870	14.254	4.967	1.36	101.68

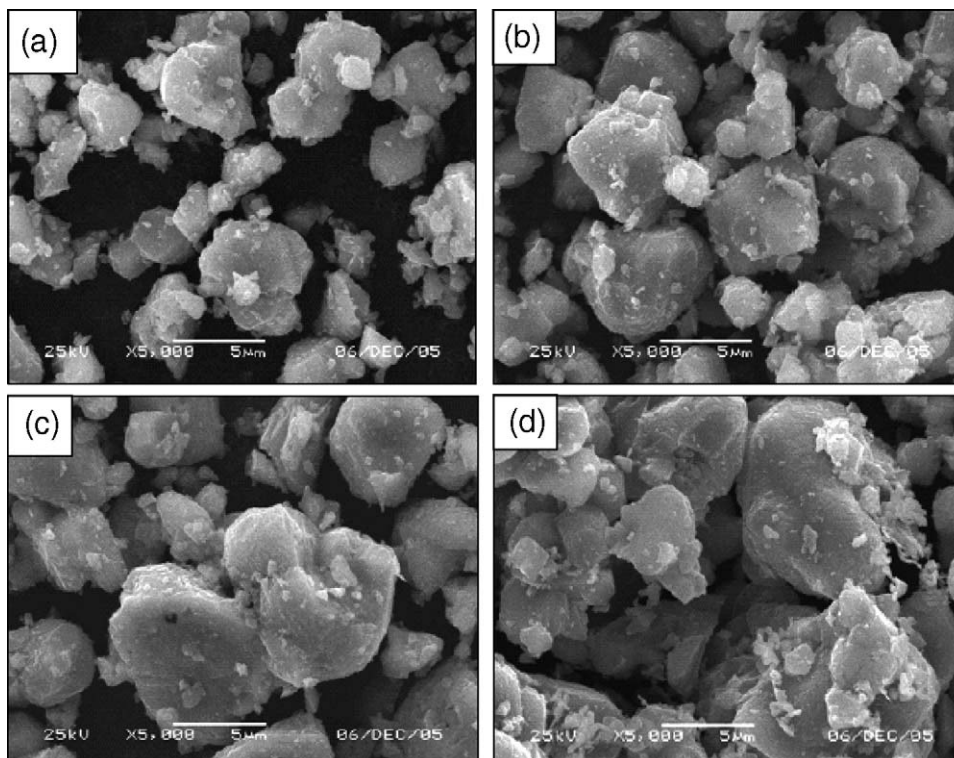


Fig. 2. SEM photographs of $\text{Li}[\text{Ni}_{0.333}\text{Co}_{0.333}\text{Mn}_{0.293}\text{Al}_{0.04}]\text{O}_{2-z}\text{F}_z$. (a) $z=0$; (b) $z=0.02$; (c) $z=0.05$; (d) $z=0.1$.

substitution of fluorine resulted in the partial reduction of the transition metal ions for the charge compensation of F anions. As the radii of Mn^{3+} (0.645 Å) is larger than Mn^{4+} (0.53 Å) and Co^{2+} (0.65 Å) is larger than Co^{3+} (0.545 Å), it led to the increase in both a - and c -axis [9]. The c/a ratio slightly decreased from 4.979 for $z=0$ to 4.967 for $z=0.1$, which indicates that a disordered phase with more lithium deficiency will be formed with increasing z -values. Above all, the results clearly confirmed that fluorine ions were successfully substituted for oxygen ions in the $\text{Li}(\text{Ni}_{1/3}\text{Co}_{1/3}\text{Mn}_{1/3})\text{O}_2$ crystal.

The morphologies of the synthesized $\text{Li}[\text{Ni}_{0.333}\text{Co}_{0.333}\text{Mn}_{0.293}\text{Al}_{0.04}]\text{O}_{2-z}\text{F}_z$ ($0 \leq z \leq 0.1$) powder were observed using SEM and are shown in Fig. 2. It can be seen from the SEM images that $\text{Li}[\text{Ni}_{0.333}\text{Co}_{0.333}\text{Mn}_{0.293}\text{Al}_{0.04}]\text{O}_2$ had a small particle size and an agglomerated morphology. As the fluorine content increased, the particle size increased from 2 to 8 μm in diameter. A similar morphological change was previously reported in the F-doped LiMn_2O_4 system [22,23]. It is well known that LiF is an effective mineralizing agent, the small quantity of LiF could accelerate the crystal growth of spinel powders with an enlarged particle size. This indicates that the particle shape and size of the as-prepared powders could be controlled by the doped fluorine content. Thus, these results suggest that the well-developed crystal structure and uniform particle size distribution of $\text{Li}[\text{Ni}_{0.333}\text{Co}_{0.333}\text{Mn}_{0.293}\text{Al}_{0.04}]\text{O}_{2-z}\text{F}_z$ could be synthesized by the sol-gel process. The regular morphology of the synthesized powders is expected to improve the electrochemical properties, resulting in high specific capacity and good cyclability.

In order to study the influence of Al-F co-substitution on the electrochemical performance, the cells were operated at a charge/discharge current density of $16 \text{ mA}^{-1} \text{ g}$ at room temperature. Fig. 3 shows the initial charge–discharge profile of the $\text{Li}[\text{Ni}_{0.333}\text{Co}_{0.333}\text{Mn}_{0.293}\text{Al}_{0.04}]\text{O}_{2-z}\text{F}_z$ ($0 \leq z \leq 0.1$) powder. Charge–discharge capacity and capacity retention ratio of the samples are tabulated in Table 2. As can be seen from the figures, all cells showed quite smooth and monotonous charge/discharge curves. On charging at $16 \text{ mA}^{-1} \text{ g}$, the voltage suddenly increased to about 3.6 V and held at 3.6–3.8 V until the charge capacity reached about $90 \text{ mAh}^{-1} \text{ g}$, which could be attributed to the $\text{Ni}^{2+}/\text{Ni}^{3+}$ redox reaction occurred in this

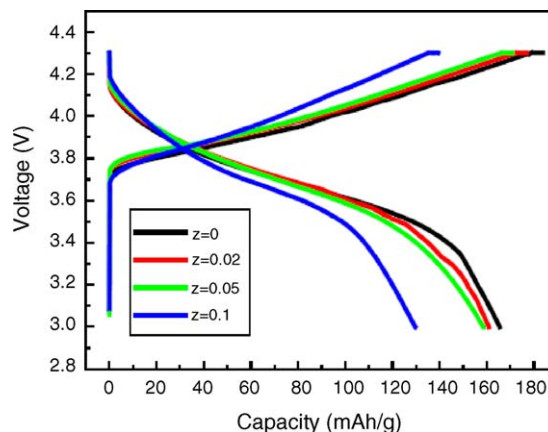


Fig. 3. Initial charge–discharge profile of $\text{Li}[\text{Ni}_{0.333}\text{Co}_{0.333}\text{Mn}_{0.293}\text{Al}_{0.04}]\text{O}_{2-z}\text{F}_z$, operated at $16 \text{ mA}^{-1} \text{ g}$ from 3 to 4.3 V.

Table 2

Charge–discharge capacity of $\text{Li}[\text{Ni}_{0.333}\text{Co}_{0.333}\text{Mn}_{0.293}\text{Al}_{0.04}]\text{O}_{2-z}\text{F}_z$

z	First charge capacity (mAh^{-1}g)	First discharge capacity (mAh^{-1}g)	First loss capacity (mAh^{-1}g)	First discharge efficiency (%)	20th discharge capacity (mAh^{-1}g)	20th capacity retention (%)
0	184	165	19	90.1	143	84.6
0.02	177	161	15	91.0	145	90.1
0.05	171	158	13	92.4	150	94.9
0.1	139	130	9	93.1	127	97.7

region [2]. And then the voltage curves monotonously increased to 4.3 V, which was similar to that observed by Ohzuku and co-workers [6]. The F-free $\text{Li}[\text{Ni}_{0.333}\text{Co}_{0.333}\text{Mn}_{0.293}\text{Al}_{0.04}]\text{O}_{2-z}\text{F}_z$ ($z=0$) electrodes showed a charge capacity of $184\text{mAh}^{-1}\text{g}$ and discharge capacity of $165\text{mAh}^{-1}\text{g}$ in the initial cycle, for which the efficiency corresponds to 90.1%. The obtained capacity was considerably higher than that of $\text{Li}(\text{Ni}_{1/3}\text{Co}_{1/3}\text{Mn}_{1/3})\text{O}_2$ obtained by Kobayashi et al. ($160\text{mAh}^{-1}\text{g}$) based on the cut-off voltages of 2.5–4.6 V. As the fluorine content increased, the discharge capacities were decreased. The discharge capacity of 161, 158 and $130\text{mAh}^{-1}\text{g}$, respectively, were obtained at the first cycle for $z=0.02, 0.05, 0.1$. However, the coulombic efficiencies were greatly improved with the increase in fluorine content. Maybe a strong covalent of Li–F exists in $\text{Li}[\text{Ni}_{0.333}\text{Co}_{0.333}\text{Mn}_{0.293}\text{Al}_{0.04}]\text{O}_{2-z}\text{F}_z$ so that intercalation of Li^+ ions will be perturbed by the strong bond, which led to the decrease of initial capacity [9].

As was reported [7], when the cell was charged over 4.3 V, the electrolyte is decomposed, which can cause safety problems. However, in the above results, although the charge/discharge processes of batteries were conducted from 3.0 to 4.3 V, the capacity of the battery with the Al–F co-doped samples as cathode-active material was similar to that of $\text{Li}(\text{Ni}_{1/3}\text{Co}_{1/3}\text{Mn}_{1/3})\text{O}_2$ obtained between 2.5–4.6 V. Consequently, Al–F co-substitution can effectively inhibit decomposition of the electrolyte and improve the safety of the batteries.

Fig. 4 compares the discharge capacity with cycle number of the $\text{Li}[\text{Ni}_{0.333}\text{Co}_{0.333}\text{Mn}_{0.293}\text{Al}_{0.04}]\text{O}_{2-z}\text{F}_z$ ($0 \leq z \leq 0.1$) powder for different content of fluorine. Although the F-free $\text{Li}[\text{Ni}_{0.333}\text{Co}_{0.333}\text{Mn}_{0.293}\text{Al}_{0.04}]\text{O}_{2-z}\text{F}_z$ ($z=0$) electrodes had the highest initial discharge capacity, they showed abrupt

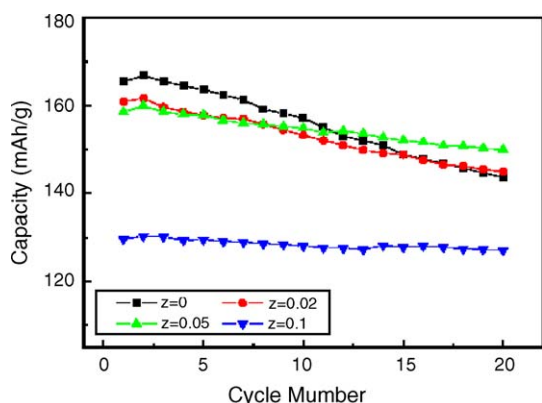


Fig. 4. Discharge capacity vs. cycle number of $\text{Li}[\text{Ni}_{0.333}\text{Co}_{0.333}\text{Mn}_{0.293}\text{Al}_{0.04}]\text{O}_{2-z}\text{F}_z$, operated at 0.1 C rate from 3 to 4.3 V at room temperature.

decrease in capacity during cycling and the capacity retention was 84.6% at the 20th cycle. On the contrary, the F-doped samples showed better cycle performance though they had lower initial capacities. Among the F-doped samples, $\text{Li}[\text{Ni}_{0.333}\text{Co}_{0.333}\text{Mn}_{0.293}\text{Al}_{0.04}]\text{O}_{1.95}\text{F}_{0.05}$ displayed the highest discharge capacity and had no significant capacity loss during cycling. The discharge capacity reached $150\text{mAh}^{-1}\text{g}$ and the capacity retention was 94.9% at the 20th cycle. Moreover, as we can see after 13 cycles, the obtained discharge capacity of $\text{Li}[\text{Ni}_{0.333}\text{Co}_{0.333}\text{Mn}_{0.293}\text{Al}_{0.04}]\text{O}_{1.95}\text{F}_{0.05}$ was even higher than that of the F-free sample. From these results, Al–F co-doping of $\text{Li}(\text{Ni}_{1/3}\text{Co}_{1/3}\text{Mn}_{1/3})\text{O}_2$ is an effective means to substantially enhance cyclability during cycling, and $\text{Li}[\text{Ni}_{0.333}\text{Co}_{0.333}\text{Mn}_{0.293}\text{Al}_{0.04}]\text{O}_{1.95}\text{F}_{0.05}$ has good electrochemical performance for lithium ion batteries.

4. Conclusions

Al–F co-substituted layered $\text{Li}[\text{Ni}_{0.333}\text{Co}_{0.333}\text{Mn}_{0.293}\text{Al}_{0.04}]\text{O}_{2-z}\text{F}_z$ ($0 \leq z \leq 0.1$) materials have been successfully synthesized by the sol–gel process. All samples had a hexagonal $\alpha\text{-NaFeO}_2$ structure and no impurity-related peaks. As the fluorine content increased, the lattice parameters increased monotonously. The particle size of $\text{Li}[\text{Ni}_{0.333}\text{Co}_{0.333}\text{Mn}_{0.293}\text{Al}_{0.04}]\text{O}_{2-z}\text{F}_z$ tended to increase with increasing z -values.

The $\text{Li}[\text{Ni}_{0.333}\text{Co}_{0.333}\text{Mn}_{0.293}\text{Al}_{0.04}]\text{O}_{2-z}\text{F}_z$ ($0 \leq z \leq 0.1$) materials showed good electrochemical performance. Though the F-doped samples had lower initial capacities, they showed better cycle performance compared to the F-free sample. The $\text{Li}[\text{Ni}_{0.333}\text{Co}_{0.333}\text{Mn}_{0.293}\text{Al}_{0.04}]\text{O}_{1.95}\text{F}_{0.05}$ electrode delivers an initial discharge capacity of $158\text{mAh}^{-1}\text{g}$ between 3 and 4.3 V at a current density of $16\text{mA}^{-1}\text{g}$ at room temperature, and the capacity retention at the 20th cycle was 94.9%. The outstanding electrochemical properties of $\text{Li}[\text{Ni}_{0.333}\text{Co}_{0.333}\text{Mn}_{0.293}\text{Al}_{0.04}]\text{O}_{1.95}\text{F}_{0.05}$ make it a promising cathode material for lithium-ion batteries.

Acknowledgements

The authors are thankful for the support provided by the Key Project of Department of Science and Technology of Hunan Province under the grant No. 05GK2015, the Key Project of Department of Education of Hunan Province under the grant No. 04A054, and the Key Project of Ministry of Education of China under the grant No. 205109.

References

- [1] N. Yabuuchi, T. Ohzuku, J. Power Sources 119–121 (2003) 171–174.
- [2] D.C. Li, T. Muta, L.Q. Zhang, M. Yoshio, H. Noguchi, J. Power Sources 132 (2004) 150–155.
- [3] M.H. Lee, Y.J. Kang, S.T. Myung, Y.K. Sun, Electrochim. Acta 50 (2004) 939–948.
- [4] T.H. Cho, S.M. Park, M. Yoshi, T. Hirai, Y. Hideshima, J. Power Sources 142 (2005) 306–312.
- [5] M.G. Kim, H.J. Shin, J.H. Kim, S.H. Park, Y.K. Sun, J. Electrochem. Soc. 152 (2005) A1320–A1328.
- [6] T. Ohzuku, Y. Makimura, Chem. Lett. 7 (2001) 642–643.
- [7] K.M. Shaju, G.V. Subba Rao, B.V.R. Chowdari, Electrochim. Acta 48 (2002) 145–151.
- [8] G.H. Kim, S.T. Myung, H.S. Kim, Y.K. Sun, Electrochim. Acta 68 (2005) 1584–1590.
- [9] G.H. Kim, S.T. Myung, H.S. Kim, C.S. Yoon, Y.K. Sun, J. Electrochem. Soc. 152 (2005) A1707–A1713.
- [10] S.H. Park, S.W. Oh, Y.K. Sun, J. Power Sources 146 (2005) 622–625.
- [11] S.H. Na, H.S. Kim, S.I. Kim, Solid State Ionics 176 (2005) 313–317.
- [12] S. Jouanneau, J.R. Dahn, J. Electrochem. Soc. 151 (2004) A1749–A1754.
- [13] G.H. Kim, S.T. Myung, H.J. Bang, J. Prakash, Y.K. Sun, Electrochem. Solid-State Lett. 7 (2004) A477–A480.
- [14] S.H. Park, C.S. Yoon, S.G. Kang, H.S. Kim, S.I. Moon, Y.K. Sun, Electrochim. Acta 49 (2004) 557–563.
- [15] P.S. Whitfield, I.J. Davidson, L.M.D. Cranswick, I.P. Swainson, P.W. Stephens, Solid State Ionics 176 (2005) 463–471.
- [16] X. Luo, X. Wang, L. Liao, S. Gamboa, P.J. Sebastian, J. Power Sources 158 (2006) 654–658.
- [17] Z. Lu, D.D. MacNeil, J.R. Dahn, Electrochem. Solid-State Lett. 4 (2001) A200–A203.
- [18] D.D. MacNeil, Z. Lu, J.R. Dahn, J. Electrochem. Soc. 149 (2002) A1332–A1336.
- [19] S.C. Garcia, A.C. Couceiro, M.A.S. Rodriguez, F. Soulette, C. Julien, Solid State Ionics 156 (2003) 15–26.
- [20] Z. Wang, Y. Sun, L. Chen, X. Huang, J. Electrochem. Soc. 151 (2004) A914–A921.
- [21] D.G. Tong, Q.Y. Lai, N.N. Wei, A.D. Tang, L.X. Tang, K.L. Huang, X.Y. Ji, Mater. Chem. Phys 94 (2005) 423–428.
- [22] G.G. Amatucci, N. Pereira, T. Zhang, J.M. Tarascon, J. Power Sources 81–82 (2004) 39–43.
- [23] M.R. Palacin, F.L. Cras, J. Seguin, M. Anne, Y. Chabre, J.M. Tarascon, G. Amatucci, G. Vaughan, J. Solid State Chem. 144 (1999) 361–371.